PHOTONICS Research

Controllable shaping of high-index dielectric nanoparticles by exploiting the giant optical force of femtosecond laser pulses

Yuheng Mao,[1,†] Shuwen Bai,[2,†] Mingcheng Panmai,[1] Lidan Zhou,[1,3] Shimei Liu,[1] Shulei Li,[4] Haiying Liu,[1] Haihua Fan,[1] Jun Dai,[4] and Sheng Lan[1,*]

[1]Guangdong Provincial Key Laboratory of Nanophotonic Functional Materials and Devices, School of Information and Optoelectronic Science and Engineering, South China Normal University, Guangzhou 510006, China
[2]Shenzhen Institute of Terahertz Technology and Innovation, Shenzhen 518102, China
[3]State Key Laboratory of Optoelectronic Materials and Technologies, School of Electronics and Information Technology, Sun Yat-sen University, Guangzhou 510006, China
[4]School of Optoelectronic Engineering, Guangdong Polytechnic Normal University, Guangzhou 510665, China
[†]These authors contributed equally to this work.
*Corresponding author: slan@scnu.edu.cn

Received 24 August 2023; revised 26 November 2023; accepted 5 December 2023; posted 6 December 2023 (Doc. ID 503661); published 1 February 2024

Nanoparticles made of different materials usually support optical resonances in the visible to near infrared spectral range, such as the localized surface plasmons observed in metallic nanoparticles and the Mie resonances observed in dielectric ones. Such optical resonances, which are important for practical applications, depend strongly on the morphologies of nanoparticles. Laser irradiation is a simple but effective way to modify such optical resonances through the change in the morphology of a nanoparticle. Although laser-induced shaping of metallic nanoparticles has been successfully demonstrated, it remains a big challenge for dielectric nanoparticles due to their larger Young's modulus and smaller thermal conductivities. Here, we proposed and demonstrated a strategy for realizing controllable shaping of high-index dielectric nanoparticles by exploiting the giant optical force induced by femtosecond laser pulses. It was found that both Si and Ge nanoparticles can be lit up by resonantly exciting the optical resonances with femtosecond laser pulses, leading to the luminescence burst when the laser power exceeds a threshold. In addition, the morphologies of Si and Ge nanoparticles can be modified by utilizing the giant absorption force exerted on them and the reduced Young's modulus at high temperatures. The shape transformation from sphere to ellipsoid can be realized by laser irradiation, leading to the blueshifts of the optical resonances. It was found that Si and Ge nanoparticles were generally elongated along the direction parallel to the polarization of the laser light. Controllable shaping of Si and Ge can be achieved by deliberately adjusting the excitation wavelength and the laser power. Our findings are helpful for understanding the giant absorption force of femtosecond laser light and are useful for designing nanoscale photonic devices based on shaped high-index nanoparticles.

https://doi.org/10.1364/PRJ.503661

1. INTRODUCTION

In ancient times, people made farm tools and weapons by hitting iron that had been heated to a high temperature. In this case, the Young's modulus of iron is reduced at high temperatures so that it can be readily shaped by hitting. As compared with metals, dielectric materials usually possess higher melting temperatures and larger Young's moduli. As a result, they are difficult to shape. For example, it is necessary to heat glass to a temperature as high as ~1700 K in order to make a glass vessel.

Since the invention of the laser in 1960s, human life has been significantly changed by laser light. Nowadays, picosecond and femtosecond lasers have been widely used in the cutting, welding, and molding of metals by exploiting the photon energy carried by the laser light. In the micro- or mesoscopic world, laser light is also employed to excite [1–4], manipulate, and shape [5–9] metallic micro- and nanoparticles. It is well known that metallic nanoparticles usually support localized surface plasmon resonances (LSPRs) in the visible to near infrared spectral range, which depend strongly on the morphologies of nanoparticles. Therefore, the LSPR of a metallic nanoparticle, at which the electric field is greatly enhanced, can be modified by changing the shape of the nanoparticle. The modification of the LSPR of

a metallic nanoparticle is generally accompanied by the change in the color of the scattering light of the nanoparticle. This feature has been exploited to realize nanoscale color display with laser-shaped metallic nanoparticles [10]. In most cases, shaping of metallic nanoparticles by laser irradiation is realized by exploiting the heat released by the non-radiative recombination of photo-generated carriers. In comparison, less attention has been paid to the optical force exerted on nanoparticles by laser light. It is well known that a laser beam can be employed to manipulate a nanoparticle by exploiting the optical force acting on the nanoparticle. It was demonstrated that a metallic nanoparticle can be shaped by a continuous wave laser light, leading to the color change in the scattering light [5,7,8].

Dielectric nanoparticles with high refractive indices, such as silicon (Si), germanium (Ge), and gallium arsenide (GaAs) nanoparticles, support distinct Mie resonances in the visible to near infrared spectral range. They are considered as artificial atoms for constructing metasurfaces and metamaterials operating at optical frequencies. Similar to their metallic counterparts, the Mie resonances supported in a dielectric nanoparticle depend strongly on the morphology of the nanoparticle. It implies that one can modify the wavelengths of these optical resonances by shaping the dielectric nanoparticle. In a previous study, it was shown by numerical simulation that an ellipsoidal Si nanoparticle exhibits a distinct magnetic quadrupole (MQ) resonance well separated from the electric dipole (ED) one [11]. Comparing with the MQ of a spherical Si nanoparticle, it is revealed that the MQ of the ellipsoidal Si nanoparticle will offer larger two-photon-induced absorption (TPA) when it is resonantly excited by femtosecond laser pulses [12]. It means that shaping of dielectric nanoparticles is also desirable from the viewpoint of practical applications. In recent studies, spherical Si nanoparticles made by femtosecond laser ablation were usually used to construct Si/Au nanocavities with an embedded WS_2 monolayer for investigating plasmon-exciton coupling [13–15]. In this case, it is highly desirable that the optical resonance of a Si/Au nanocavity, which is determined by the size and shape of the Si nanoparticle, can match the exciton resonance of WS_2 monolayer. In this regard, laser-induced shaping of Si nanoparticles appears as a simple and effective way to achieve this goal.

As mentioned at the beginning, dielectric materials usually possess a higher melting point and smaller thermal conductivity as compared with metals. In addition, the absorption of such dielectric materials in the visible to near infrared spectral range is also much smaller in comparison with metals. Otherwise, they cannot support distinct Mie resonances. Therefore, it remains a big challenge to realize controllable shaping of dielectric nanoparticles by using femtosecond laser light.

In this work, we investigated the shaping of Si and Ge nanoparticles placed on ITO/SiO_2 and Au/SiO_2 substrates by femtosecond laser pulses. We demonstrated that high-index nanoparticles made of semiconductors with indirect bandgaps can be lit up by resonantly exciting the optical resonances with femtosecond laser pulses. It was observed that the burst of hot electron luminescence can be induced by raising the laser power above a threshold. The Young's modulus of Si or Ge reduced at high temperatures when the burst of luminescence occurred. It was found that a spherical nanoparticle can be transformed into an ellipsoidal one with its long axis parallel to the polarization of the laser light by irradiating the nanoparticle with laser light above the threshold. The shaping of a dielectric nanoparticle depends not only on the melting point and Young's modulus of the dielectric material but also on the substrate used to support the nanoparticle.

2. RESULTS AND DISCUSSION

A. Shaping of Si Nanoparticles by Femtosecond Laser Pulses

In Fig. 1, we show schematically the morphology change induced by femtosecond laser pulses in a Si (or Ge) nanoparticle placed on an ITO/SiO_2 or an Au/SiO_2 substrate. Since the nonlinear optical absorption (e.g., TPA) at the optical resonances of the Si (or Ge) nanoparticle is greatly enhanced, high-density carriers can be injected into the Si (or Ge) nanoparticle through the resonant excitation of the optical resonances by using femtosecond laser pulses. If the excitation laser power exceeds a critical value (i.e., a threshold), the heat released from the thermalization of hot carriers will heat the Si (or Ge) nanoparticle to a high temperature at which the intrinsic excitation of carriers occurs. As a result, one can observe the burst of hot electron luminescence from the Si (or Ge) nanoparticle [16–20].

In previous studies, much effort was devoted to enhancing the quantum efficiency of the hot electron luminescence [1,2,16–22]. In comparison, less attention was paid to the morphology change of the nanoparticle induced by femtosecond laser pulses. Since the first demonstration of the optical tweezer in 1980s by Ashkin, the gradient force generated by a focused continuous wave (CW) laser beam is commonly employed to manipulate micro- and nanoparticles [5,8,23,24]. However, very few studies have been devoted to the optical forces generated by femtosecond laser light, which are associated with nonlinear optical effects [18,25]. Apart from scattering and gradient forces, the absorption force induced by femtosecond laser light can be very huge if the nonlinear optical absorption of a nanoparticle is great. In this case, the momentum carried by the photons of the femtosecond laser light will be converted to the optical force exerted on the nanoparticle in an ultrashort time (~100 fs), resulting in a giant optical force acting on the nanoparticle. On the other hand, the dielectric nanoparticle (Si or Ge) will become softer at high temperatures due to the reduced Young's modulus. Physically, the circular electric field distribution at the MD resonance provides highly efficient nonlinear optical absorption, which is employed to inject high-density carriers into a nanoparticle and to generate giant absorption force acting on the nanoparticle. Based on a previous study [12], the high-order Mie resonances supported by a Si nanoparticle can also be employed to achieve enhanced nonlinear optical absorption and emission from the Si nanoparticle. Therefore, it is expected that the resonant excitation of such optical resonances can also be used to realize the shaping of Si nanoparticles. On the other hand, it was reported that structured light will offer enhanced nonlinear optical efficiency due to the match between the electric field of the light and the mode pattern of the nanoparticle [26]. Thus, lighting and

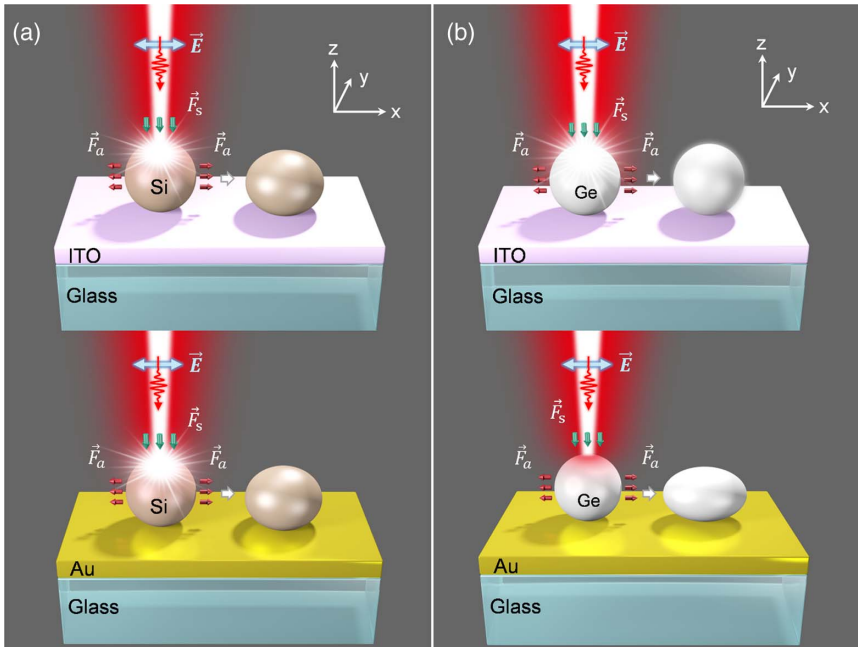

Fig. 1. (a) Schematic showing the controllable shaping of a spherical Si nanoparticle placed on an ITO/SiO_2 or an Au/SiO_2 substrate into an ellipsoidal one by using femtosecond laser pulses. (b) Schematic showing the controllable transformation of a spherical Ge nanoparticle placed on an Au/SiO_2 substrate into an ellipsoidal one by using femtosecond laser pulses. A spherical Ge nanoparticle placed on an ITO/SiO_2 substrate cannot be shaped by femtosecond laser pulses because of melting of the Ge nanoparticle.

shaping high-index dielectric nanoparticles by using structured light is an interesting topic to be investigated in the future [27]. Therefore, a morphology change is expected to occur for the nanoparticle once it is lit up by femtosecond laser light. As demonstrated later, spherical Si nanoparticles can be shaped into ellipsoidal ones no matter if they are placed on an ITO/SiO_2 substrate or an Au/SiO_2 substrate. In comparison, spherical Ge nanoparticles can only be transformed into ellipsoidal ones when they are placed on an Au/SiO_2 substrate. In both cases, it was found that the long axes of shaped Si or Ge nanoparticles are parallel to the polarization of the femtosecond laser light.

In Fig. 2(a), we show the evolution of the luminescence spectrum of a Si nanoparticle placed on an ITO/SiO_2 substrate with increasing excitation laser power (P). In this case, an 800 nm femtosecond laser beam polarized along the x direction was employed to excite the Si nanoparticle. It can be seen that the luminescence burst occurs at $P = 12$ mW. In Fig. 2(b), we present the scattering spectra of the Si nanoparticle measured before and after the luminescence burst. In both cases, one can identify the electric dipole (ED) and magnetic dipole (MD) resonances supported by the Si nanoparticle. It is noticed, however, that the MD resonance is shifted to a shorter wavelength after the luminescence burst. In comparison, the ED resonance remains nearly unchanged. It is noticed that the MQ resonance, which is initially hidden in the broad ED resonance, emerges in the scattering spectrum due to a blueshift. This behavior is similar to that predicted in the numerical simulation [11]. We examined the morphologies of the Si nanoparticle before and after the laser irradiation based on scanning electron microscopy (SEM) observation, as shown in the insets of Fig. 2(b). From the top view of the Si nanoparticle, it was found that the Si nanoparticle was elongated along the polarization of the laser light, which was set in the x direction. We also examined another Si nanoparticle, which was excited by using 800 nm femtosecond laser light polarized along the y direction. Similarly, we observed the luminescence burst when the laser power reached $P = 12$ mW, as shown in Fig. 2(c). The modification in the scattering spectrum of the Si nanoparticle is quite similar to that observed for the previous one, as shown in Fig. 2(d). However, it was found that the Si nanoparticle was elongated along the y direction after the luminescence burst, which was the polarization direction of the laser light. This behavior implies that the deformation of the Si nanoparticle is closely related to the polarization of the laser light.

Physically, the change in the scattering spectrum of the Si nanoparticle may originate from the modification in the structure or morphology of the Si nanoparticle. In order to clarify this point, we performed numerical simulations for the scattering spectra of Si@SiO_2 core-shell structures and ellipsoidal Si nanoparticles with different dimensions in the z direction. It was found that the change in the scattering spectrum cannot be attributed to the oxidation of the Si nanoparticle. Instead, the morphological change of the Si nanoparticle from sphere to ellipsoid, which was also verified by the SEM images, can reproduce the scattering spectrum of the Si nanoparticle observed in the experiments. In Fig. 2(e), we present the two-dimensional scattering spectra simulated for ellipsoidal Si nanoparticles with different diameters in the z direction (d_z), in which the evolutions of the MD, ED, and MQ resonances with decreasing d_z are clearly identified. Although we had only

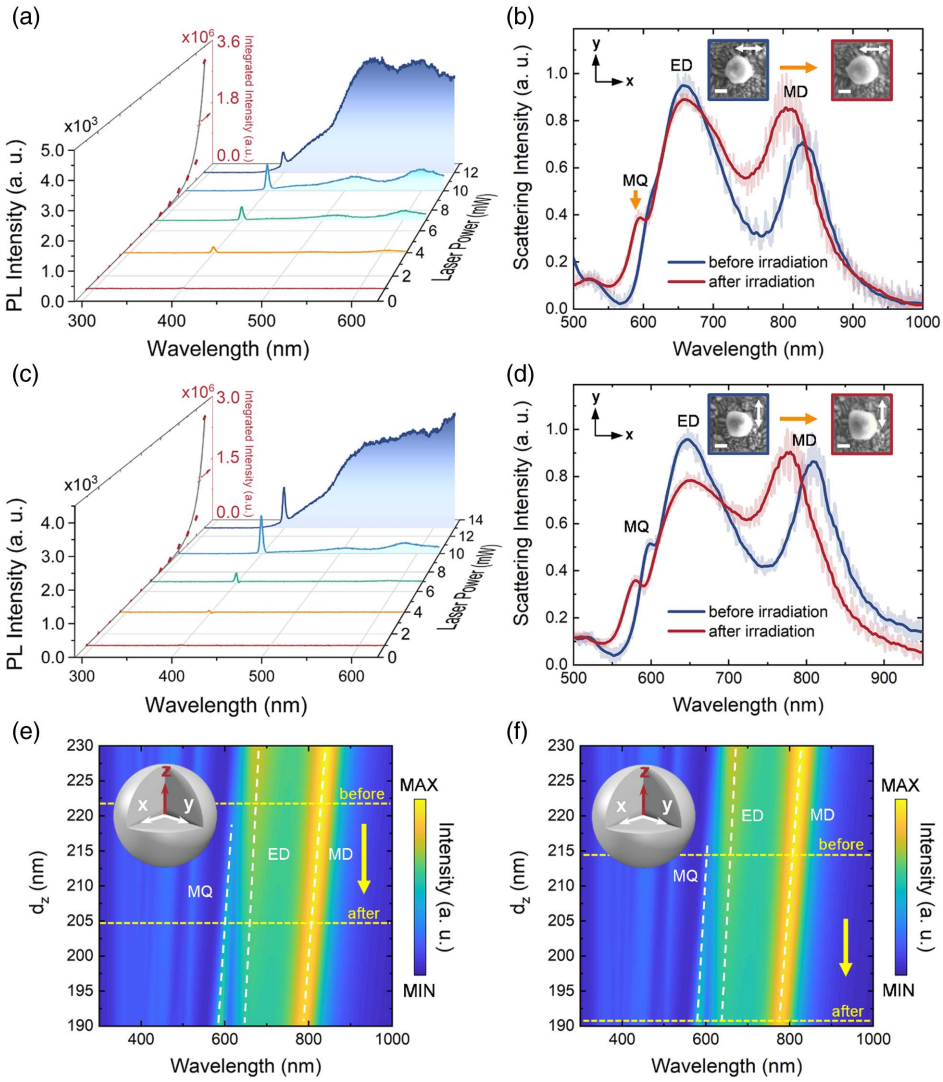

Fig. 2. (a) Evolution of the luminescence spectrum with increasing laser power measured for a Si nanoparticle (particle A). (b) Scattering spectra measured for a Si nanoparticle (particle A) before and after the laser irradiation above the threshold. The SEM images before and after the laser irradiation are shown as insets. The polarization of the laser light is indicated by arrows. The length of the scale bar is 100 nm. (c) Evolution of the luminescence spectrum with increasing laser power measured for another Si nanoparticle (particle B). (d) Scattering spectra measured for another Si nanoparticle (particle B) before and after the laser irradiation above the threshold. The SEM images before and after the laser irradiation are shown as insets. The polarization of the laser light is indicated by arrows. The length of the scale bar is 100 nm. (e) Two-dimensional scattering spectra calculated for ellipsoidal Si nanoparticles with fixed dimensions in the XY plane ($d_x = 220$ nm, $d_y = 222$ nm) and variant dimension in the z direction ($d_z = 190$–230 nm). Measured results before and after laser irradiation are indicated with yellow dashed lines. (f) Two-dimensional scattering spectra calculated for ellipsoidal Si nanoparticles with fixed dimensions in the XY plane ($d_x = 214$ nm, $d_y = 216$ nm) and variant dimension in the z direction ($d_z = 190$–230 nm). Measured results before and after laser irradiation are indicated with yellow dashed lines.

the data for one Si nanoparticle before and after the laser irradiation, the wavelengths of the MD, ED, and MQ resonances extracted from the simulation result match well with those observed in the experimental observation [see the two dashed lines in Fig. 2(e)]. In Fig. 2(f), the evolutions of the MD, ED, and MQ resonances of a Si nanoparticle ($d_x = 214$ nm, $d_y = 216$ nm) with decreasing d_z are predicted based on numerical simulations. The two dashed lines indicate the initial and final values for d_z extracted from the scattering spectra [see Fig. 2(d)]. In our experiments, we examined the scattering spectra and morphologies of many Si nanoparticles and confirmed that Si nanoparticles can be elongated along the polarization direction of the laser light after the luminescence burst, no matter if they are placed on an ITO/SiO_2 or an Au/SiO_2 substrate.

In previous studies, we have demonstrated that Si nanoparticles can be lit up by injecting high-density carriers through resonantly exciting the optical resonances with femtosecond laser pulses [16–20]. We think that the underlying physical mechanism is applicable to other high-index dielectric nanoparticles made of semiconductors with indirect bandgaps. Consequently, high-index dielectric nanoparticles can also be shaped by utilizing the optical force of femtosecond laser pulses.

B. Lighting and Shaping of Ge Nanoparticles by Femtosecond Laser Pulses

In order to confirm this suspect, we carried out similar experiments for Ge nanoparticles placed on an ITO/SiO_2 or an Au/SiO_2 substrate by using 715 nm femtosecond laser light. In Fig. 3(a), we show the luminescence spectra measured for a Ge nanoparticle placed on the ITO/SiO_2 substrate at different laser powers. A rapid increase in the luminescence intensity is observed when the laser power exceeds $P = 3$ mW. It verifies that Ge nanoparticles can also be lit up by injecting high-density carriers. However, the ED and MD resonances in the scattering spectrum of the Ge nanoparticle remain almost unchanged, as shown in Fig. 3(b). Based on the SEM images shown in the insets, it was found that the Ge nanoparticle was melted by the high temperature, leading to a spherical shape with a smooth surface. This behavior is different from that observed for Si nanoparticles placed on the ITO/SiO_2 substrate. The reason is the much lower melting point of Ge (~1210 K) as compared with that of Si (~1683 K). We calculated the dependence of intrinsic carrier density on temperature for Ge [28]. It was found that the intrinsic carrier density increases rapidly for temperatures higher than 1200 K, which exceeds the melting point of Ge. Once a Ge nanoparticle is melted, it tends to maintain a spherical shape due to the surface tension.

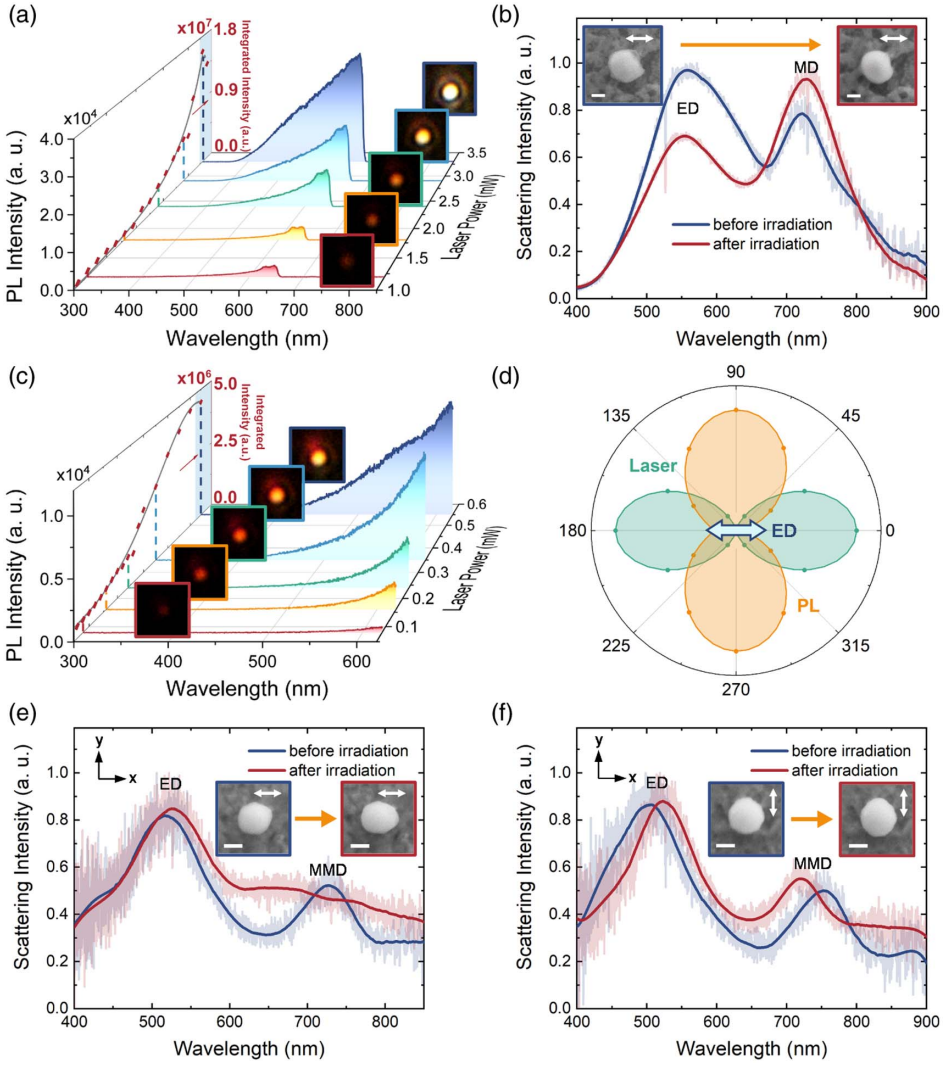

Fig. 3. (a) Evolution of the luminescence spectrum with increasing laser power measured for a Ge nanoparticle placed on an ITO/SiO_2 substrate. The luminescence images recorded by using a CCD at different laser powers are also provided. (b) Scattering spectra measured for a Ge nanoparticle placed on an ITO/SiO_2 substrate before and after the laser irradiation above the threshold. The SEM images before and after the laser irradiation are shown as insets. The length of the scale bar is 100 nm. (c) Evolution of the luminescence spectrum with increasing laser power measured for a Ge nanoparticle placed on an Au/SiO_2 substrate. The luminescence images recorded by using a CCD at different laser powers are also provided. (d) Dependence of the luminescence intensity on the polarization angle of the analyzer. The dependence of the laser light intensity on the polarization angle is also provided for reference. (e) Scattering spectra measured for a Ge nanoparticle (particle C) placed on the Au/SiO_2 substrate before and after the laser irradiation above the threshold. The SEM images before and after the laser irradiation are shown as insets. The polarization of the laser light is indicated by arrows. The length of the scale bar is 100 nm. (f) Scattering spectra measured for another Ge nanoparticle (particle D) placed on the Au/SiO_2 substrate before and after the laser irradiation above the threshold. The SEM images before and after the laser irradiation are shown as insets. The polarization of the laser light is indicated by arrows. The length of the scale bar is 100 nm.

As a result, the transformation from a sphere to an ellipsoid is not observed. Thus, the modification in the scattering spectrum of the Ge nanoparticle is expected to be small before and after the laser irradiation, as shown in Fig. 3(b).

Now we inspect the luminescence spectra measured for a Ge nanoparticle placed on an Au/SiO_2 substrate at different laser powers, as shown in Fig. 3(c). In this case, the luminescence intensity of the Ge nanoparticle increased gradually with increasing laser power. However, there was not an obvious threshold above which the luminescence burst occurs. We checked the luminescence intensity at different polarization angles by using a polarization analyzer, as shown in Fig. 3(d). It was found that the luminescence was dominated by the radiation of an ED oriented in the x direction, which is parallel to the polarization of the laser light. In this case, the hot carriers generated by the femtosecond laser light are accelerated by the electric field of the laser light, oscillating in the x direction [29]. The momentum of the free carriers is converted to the optical force acting on the nanoparticle, leading to the elongation of the nanoparticle in this direction.

Different from Ge nanoparticles placed on the ITO/SiO_2 substrate, Ge nanoparticles placed on the Au/SiO_2 substrate can be shaped by femtosecond laser light. In Figs. 3(e) and 3(f), we show the scattering spectra measured for two Ge nanoparticles before and after the laser irradiation. Before the laser irradiation, each Ge nanoparticle exhibited distinct mirror-image-induced magnetic dipole (MMD) resonance in the scattering spectrum due to the existence of the Au film [30–32]. After the laser irradiation, a blueshift of the MMD resonance was observed while the ED resonance remained almost unchanged. Based on the SEM images shown in the insets, it was found that in each case the Ge nanoparticle was elongated along the polarization of the laser light, which was intentionally set at the x and y directions, respectively. This behavior is quite similar to that observed for Si nanoparticles deformed by femtosecond laser light. For the Ge nanoparticle placed on the Au/SiO_2 substrate, the nonlinear optical absorption of the Ge nanoparticle is enhanced due to the formation of MMD resonance. In addition, the melting of the Ge nanoparticle is avoided because of the good thermal conductivity of Au.

Physically, the controllable shaping of high-index dielectric nanoparticles relies on the giant absorption force originating from the resonant excitation of the optical resonances supported by nanoparticles. The reduced Young's modulus of the material at high temperatures also plays a crucial role in the shaping of such nanoparticles. In fact, the major limitation of the method is the requirement of resonant excitation. Once a nanoparticle is deformed, the optical resonance supported by the nanoparticle will be shifted, alleviating the further shaping of the nanoparticle due to the reduced nonlinear optical absorption. Thus, it is necessary to change the wavelength of the laser light in order to achieve a large deformation of the nanoparticle. Another limitation of the method is that the shaping of a nanoparticle is influenced by the substrate used to support the nanoparticle. The Mie resonances supported by a high-index nanoparticle can be modified by the substrate [33], leading to the change in the electric field distribution, nonlinear optical absorption, and temperature distribution. On the other hand, the cooling of the shaped nanoparticle is also affected by the thermal conductivity of the substrate. When a substrate with poor thermal conductivity is used, the shaping of a nanoparticle may not be successful [e.g., Ge nanoparticles on an ITO/SiO_2 substrate; see Fig. 3(b)].

C. Optical Forces Exerted on Ge Nanoparticles by Femtosecond Laser Pulses

In order to understand the physical mechanism responsible for the shaping of Si and Ge nanoparticles, we analyzed the optical forces induced by femtosecond laser pulses and exerted on a Ge nanoparticle. In our experiments, we used 715 nm femtosecond laser light to excite the Ge nanoparticle. The energy of a single photon is $E_p = 2.78 \times 10^{-19}$ J. Based on previous studies, the density of photo-generated carriers will exceed 10^{20} cm^{-3} when the luminescence burst occurs [17]. Since carriers are injected via a TPA process, the number of photons absorbed by the Ge nanoparticle with $d = 180$ nm is estimated to be $N = 6.10 \times 10^5$, corresponding to a total energy of $E_t = 1.70 \times 10^{-13}$ J. Thus, the momentum carried by these photons is found to be $M_t = 5.70 \times 10^{-22}$ N · s. Considering that the momentum of the photons is converted to an optical force in a short time corresponding to the duration of the femtosecond laser pulses ($t = 130$ fs), the absorption force exerted on the Ge nanoparticle by a single femtosecond laser pulse is calculated to be $F_a = 4.40$ nN.

Apart from the optical force arising from the absorption of photons (an absorption force), we also calculated numerically the scattering force (radiation pressure) and gradient force exerted on the Ge nanoparticle based on the Maxwell stress tensor, as shown in Fig. 4(a) [5]. In this case, the diameter of the laser beam with a Gaussian intensity distribution was assumed to be $D = 670$ nm while the diameter of the Ge nanoparticle was chosen to be $d = 134$ nm. The maximum values for the scattering and gradient forces were found to be $F_s = 150$ fN and $F_g = 30$ fN, respectively. Apparently, they are much smaller as compared with the absorption force ($F_a = 4.40$ nN). Therefore, the shape transformation of the Ge nanoparticle is induced mainly by the absorption force of the femtosecond laser pulses, which reduces the dimension of the Ge in the vertical direction.

Due to the existence of the MMD resonance for the Ge nanoparticle placed on the Au/SiO_2 substrate, the TPA is greatly enhanced, leading to a larger absorption force exerted on the Ge nanoparticle. We calculated the temperature distributions in Ge nanoparticles placed on the ITO/SiO_2 and Au/SiO_2 substrates after the excitation of a single femtosecond laser pulse based on the two-temperature model, as shown in Fig. 4(b) [34]. It was found that the temperature distribution inside the Ge nanoparticle is not uniform in both cases. For the Ge nanoparticle placed on the ITO/SiO_2 substrate, the temperature is higher on the surface. In contrast, a higher temperature is observed at the center for the Ge nanoparticle placed on the Au/SiO_2 substrate. In addition, it was found that the temperature of the Ge nanoparticle placed on the Au/SiO_2 changes more rapidly than that of the Ge nanoparticle placed on the ITO/SiO_2 substrate due to the good thermal conductivity of Au film. Due to the enhanced TPA and increased optical force for the Ge nanoparticle on the Au/SiO_2 substrate, the

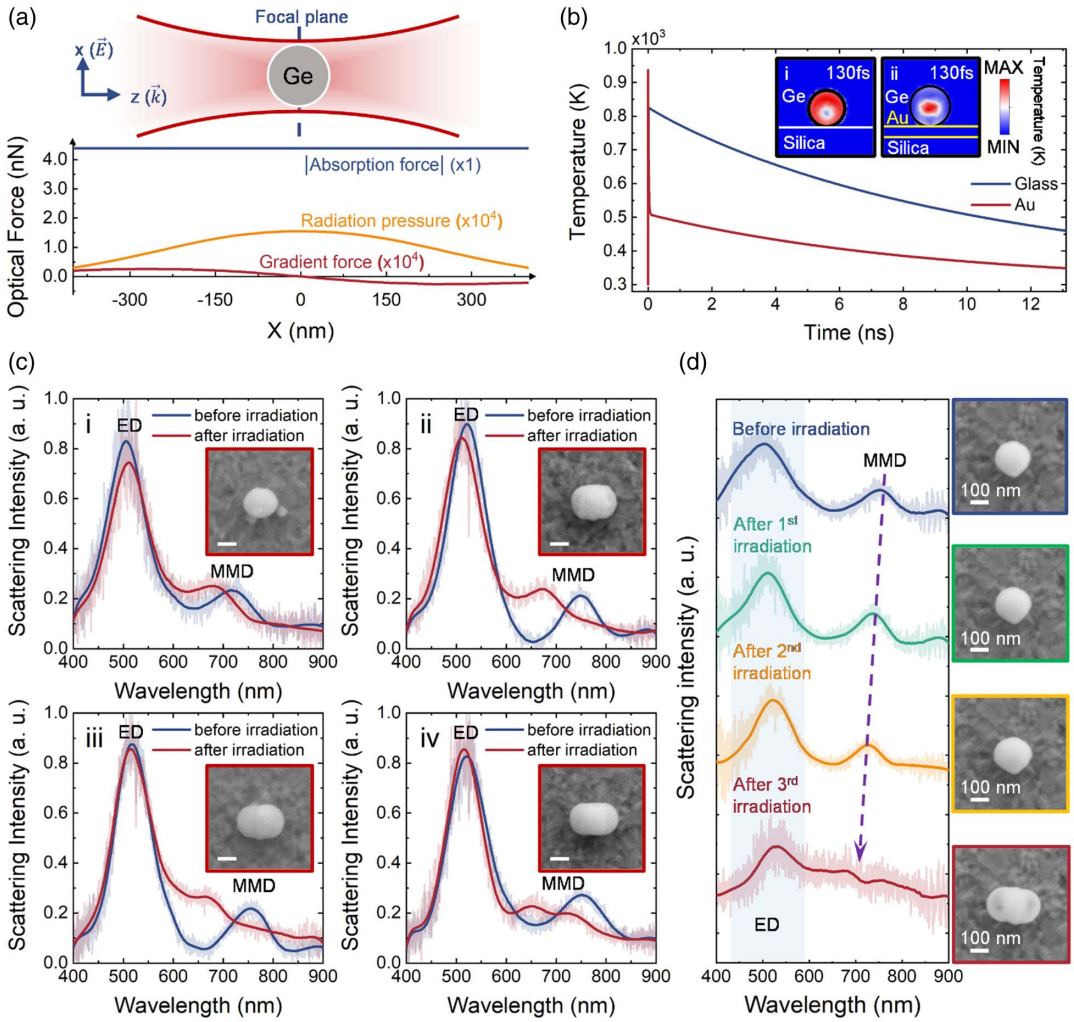

Fig. 4. (a) Optical force induced on a Ge nanoparticle by femtosecond laser pulses. (b) Evolution of the temperature calculated inside the Ge nanoparticles ($d = 134$ nm and 184 nm) placed on an ITO/SiO_2 substrate and an Au/SiO_2 substrate within one laser pulse period. Transient temperature distributions in the XZ plane (corresponding to one laser pulse excitation) calculated for a Ge nanoparticle ($d = 134$ nm and 184 nm) placed on an ITO/SiO_2 substrate and an Au/SiO_2 substrate, as shown in the insets (i) and (ii), respectively. (c) Scattering spectra measured for four different Ge nanoparticles irradiated by laser light above the threshold. The corresponding SEM images of the Ge nanoparticles are provided. The length of the scale bar is 100 nm. (d) Scattering spectra measured for a Ge nanoparticle irradiated by laser light above the threshold for different rounds. The corresponding SEM images of the Ge nanoparticle are provided.

shaping of the Ge nanoparticle occurs at a temperature lower than the melting point of Ge. Thus, we could observe an elongated Ge nanoparticle after the laser irradiation.

D. Controllable Shaping of Ge Nanoparticles by Femtosecond Laser Pulses

Since there is no luminescence burst for a Ge nanoparticle placed on the Au/SiO_2 substrate, we can achieve different degrees of deformation for the Ge nanoparticle by simply increasing the laser power. In Fig. 4(c), we present the scattering spectra measured for four Ge nanoparticles excited by using femtosecond laser light with different powers. The diameters of the Ge nanoparticles are similar before the laser irradiation. It is noticed that the blueshift of the MMD resonance after the laser irradiation becomes larger with increasing laser power. Based on the SEM images shown in the insets, it was found that the Ge nanoparticle was elongated in the direction parallel to the polarization of the laser light. More importantly, it was observed that the dimension of the ellipsoid in the x direction becomes larger with increasing laser power, in good agreement with the larger blueshift of the MMD resonance. In Fig. 4(d), we demonstrated a controllable shaping of a Ge nanoparticle by deliberately adjusting the laser power. In the first round, the excitation wavelength was chosen to be 750 nm, which was resonant with the MMD resonance of the Ge nanoparticle. The laser power was increased gradually to $P = 0.80$ mW. After the laser radiation, the MMD was shifted slightly by ~10 nm (from 750 to 740 nm). Based on the SEM image, it was found that the dimension of the Ge nanoparticle in the x direction was increased by 1.5% while that in the y direction was increased by ~1.0%. In the second round, the excitation wavelength remained unchanged, and the laser power was raised from $P = 0.80$ mW to $P = 0.96$ mW. A further blueshift

of the MMD by ~15 nm was observed. Accordingly, the dimension in the x direction was increased by ~7.5% while that in the y direction was increased by 1.5% as compared with the original values. In the third round, the excitation wavelength was set at 725 nm, and the laser power was increased from $P = 0$ to $P = 0.80$ mW. A large blueshift by ~65 nm was found for the MMD, implying a significant change in the morphology of the Ge nanoparticle. Based on the SEM observation, it was found that the Ge nanoparticle was elongated dramatically in the x direction, corresponding to a change of ~45.5% in the long axis. In comparison, the change in the short axis was much smaller (~1.5%).

In this work, we found that a high-index dielectric nanoparticle can be elongated along the polarization of the irradiation laser light. In general, the elongation of a nanoparticle occurs once it is lit up above the threshold laser power. In this case, the change in the dimension of the nanoparticle is governed mainly by the laser power used to irradiate the nanoparticle. However, the threshold laser power for lighting up a nanoparticle depends strongly on the size of the nanoparticle. By controlling the laser power, one can obtain shaped nanoparticles with different elongation rates ranging from 7.2% to 42.2% [see Fig. 4(c)]. Once the nanoparticle is deformed, the optical resonance supported by the nanoparticle is blueshifted, alleviating the further shaping of the nanoparticle. In this case, one can shape the nanoparticle again by changing the wavelength of the laser light to the new optical resonance [see Fig. 4(d)]. The change in the dimension of a nanoparticle demonstrated in this work can be as large as 45%.

Actually, realizing reversible transformation is attractive and important from the viewpoint of practical application [35]. In fact, we attempted to realize the reversible shaping of high-index nanoparticles by using a laser power much higher than the threshold. Unfortunately, we did not succeed in obtaining spherical nanoparticles although the laser power is much higher than the threshold. We also tried the reversible shaping of an ellipsoidal nanoparticle by using laser light with polarization perpendicular to the long axis of the nanoparticle. In this way, we could reduce the long axis of the ellipsoid and increase its short axis. However, the shape of the nanoparticle is different from the original one.

E. Optical Characterization of Deformed Ge Nanoparticles

As discussed above, a spherical Ge nanoparticle is generally transformed into an ellipsoidal one with its long axis along the polarization of the laser light. Basically, such a Ge nanoparticle can be characterized by using the scattering spectrum of polarized white light, as schematically shown in Fig. 5(a) [36,37]. In this case, a polarized white light beam is incident obliquely on a Ge nanoparticle sitting on the Au/SiO_2 substrate. The polarization angle of the white light can be adjusted by rotating a polarizer so that white light with different polarization angles can be generated. In Fig. 5(b), we compared the scattering spectra simulated and measured for an ellipsoidal Ge nanoparticle

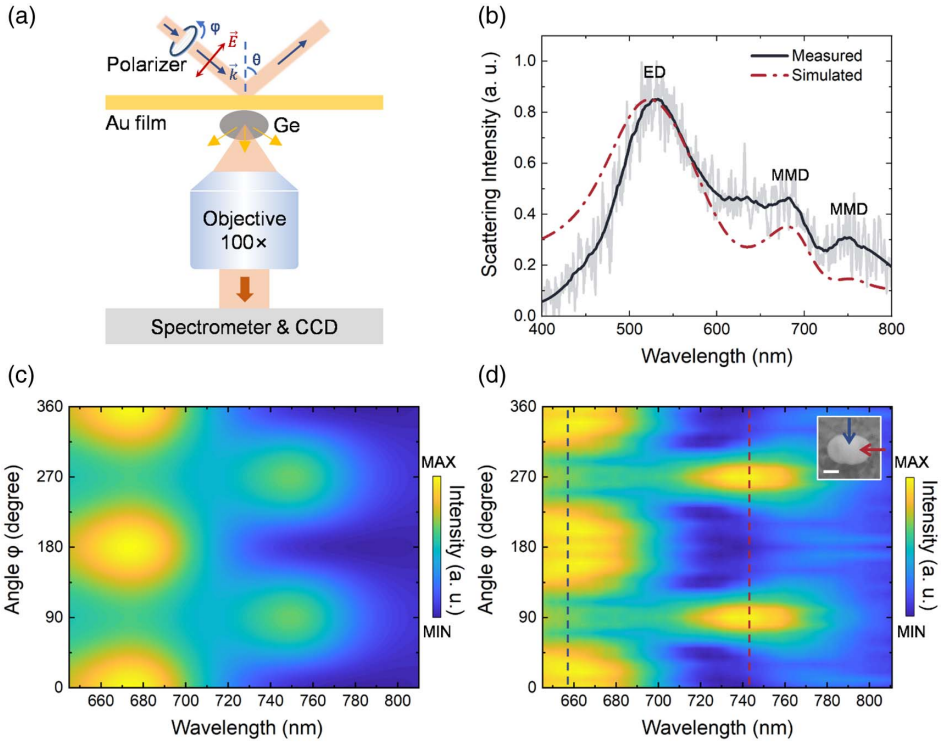

Fig. 5. (a) Schematic showing the measurements of the forward scattering spectra of a Ge nanoparticle placed on an Au/SiO_2 substrate by using polarized white light. (b) Simulated and measured scattering spectrum of an ellipsoidal Ge nanoparticle under unpolarized white light. The dimensions of the Ge nanoparticle extracted from SEM image in the x, y, and z directions are assumed to be $d_x = 293$ nm, $d_y = 220$ nm, and $d_z = 121$ nm, respectively. The simulated and measured forward scattering spectra under polarized white light with different polarization angles are shown in (c) and (d), respectively. The length of the scale bar is 100 nm.

excited by unpolarized white light. The dimensions of the Ge nanoparticle extracted from SEM image in the x, y, and z directions are assumed to be $d_x = 293$ nm, $d_y = 220$ nm, and $d_z = 121$ nm, respectively. Except the smaller scattering intensities at the short wavelengths originating from the lower efficiencies of the detector, the measured spectrum matches well with the simulated one. In Fig. 5(c), we present the two-dimensional scattering spectra simulated for the Ge nanoparticle at different polarization angles (φ) ranging from 0° to 90°. Apparently, the polarization angles of 0° and 90° correspond to s- and p-polarized light, respectively. When the Ge nanoparticle is irradiated by using s-polarized light, the ED along the y direction is excited. The ED and its mirror image create an MMD in the x direction, resulting in a peak in the scattering spectrum. Similarly, an ED along the x direction will be excited when the Ge nanoparticle is irradiated by using p-polarized light. A scattering peak resulting from the MMD in the y direction will appear in the scattering spectrum. Therefore, the ED along the long axis in the x direction and the short axis in the y direction of the ellipsoid can be excited by using p- and s-polarized light, respectively, resulting in the scattering peaks located at the long and short wavelengths. As shown in Fig. 5(c), one can see a scattering peak at ~670 nm for $\varphi = 0°$, which corresponds to the MMD induced by the s-polarized light. This scattering peak disappears at $\varphi = 90°$, and a new scattering peak emerges at ~750 nm, which corresponds to the MMD induced by the p-polarized light. In Fig. 5(d), we present the two-dimensional scattering spectra measured for the Ge nanoparticle at different polarization angles. It can be seen that the measurement results are in good agreement with the simulation ones, verifying clearly the formation of an ellipsoidal Ge nanoparticle induced by laser irradiation.

3. METHODS

A. Sample Preparation

The Si and Ge nanoparticles used in this work were fabricated by using femtosecond laser ablation. Si and Ge nanoparticles with diameters of 50–400 nm were obtained by centrifuging the aqueous solution containing Si and Ge nanoparticles at a speed of 7000 r/min. The aqueous solution was dropped and dried on an ITO/SiO_2 or an Au/SiO_2 substrate.

B. Optical Characterization

The forward scattering of Si and Ge nanoparticles was characterized by using a dark-field microscope (Observer A1, Zeiss) equipped with a charge-coupled device (CCD, DS-Ri2, Nikon) for imaging and a spectrometer (SR-500i, Andor) for spectrum analysis. The illumination light was chosen to be unpolarized or polarized white light. The femtosecond laser light with a repetition rate of 76 MHz and a duration of 130 fs was employed to excite Si and Ge nanoparticles placed on an ITO/SiO_2 or an Au/SiO_2 substrate. It was focused on Si and Ge nanoparticles by using the 100× objective lens (NA = 1.3) of an inverted microscope (Observer A1, Zeiss). The luminescence emitted from Si and Ge nanoparticles was collected by using the same objective lens and directed to a spectrometer (SR-500i, Andor) for analysis or to a CCD (DS-Ri2, Nikon) for imaging.

C. Numerical Simulation

The scattering spectrum and temperature distributions of Si and Ge nanoparticles placed on an ITO/SiO_2 or an Au/SiO_2 substrate were calculated numerically by using a commercially developed software (COMSOL Multiphysics v5.4) or with the finite-difference time-domain (FDTD) method by using a commercially developed software (FDTD solution). The numerical simulations were performed in a region whose diameter was set to be the wavelength of the incident light. The Si and Ge nanoparticles were placed at the center of a sphere, which was enclosed by a perfectly matched layer capable of absorbing all the outgoing radiation.

4. CONCLUSION

In summary, we have investigated the shaping of Si and Ge nanoparticles by exploiting the optical forces generated by femtosecond laser pulses. It was found that both Si and Ge nanoparticles can be lit up by resonantly exciting the optical resonances with femtosecond laser pulses, leading to the luminescence burst when the laser power exceeds a threshold. In addition, the morphologies of Si and Ge nanoparticles can be modified. The key point for realizing the controllable shaping of a high-index dielectric nanoparticle is injecting high-density carriers into the nanoparticle through resonantly exciting the optical resonances supported by the nanoparticle, which generates a giant absorption force. As a result, the Young's modulus of the material will be reduced at the high temperature induced by the thermalization of hot carriers, facilitating the deformation of the nanoparticle. In addition, the fast cooling of the shaped nanoparticle is also important, and it can be achieved by using a thin metal film with good thermal conductivity as the substrate for the nanoparticle. It was found that Si and Ge nanoparticles were generally elongated along the direction parallel to the polarization of the laser light. Controllable shaping of Si and Ge can be achieved by deliberately adjusting the excitation wavelength and the laser power. The shape transformation from the sphere to ellipsoid can be realized by laser irradiation, leading to the blueshifts of the optical resonances. The controllable shaping of a high-index dielectric nanoparticle demonstrated in this work can be used to realize the continuous tuning of the optical resonance supported by the nanoparticle. By inserting a two-dimensional material, the dielectric-metal hybrid nanocavity created by combining such a nanoparticle and a thin metal film can be employed to investigate strong plasmon-exciton coupling when the optical resonance of the nanocavity matches the exciton resonance in the two-dimensional material. In addition, the color change in the scattering light of the nanoparticle induced by the controllable shaping may find applications in nanoscale color display. Our findings are helpful for understanding the giant absorption force of femtosecond laser light and useful for designing nanoscale photonic devices based on shaped high-index nanoparticles.

Funding. National Natural Science Foundation of China (12174123).

Acknowledgment. The authors acknowledge the financial support from the National Natural Science Foundation of China.

Disclosures. The authors declare no conflicts of interest.

Data Availability. The data and further information that support the findings of this study are available from the corresponding author upon reasonable request.

REFERENCES

1. G. T. Boyd, Z. H. Yu, and Y. R. Shen, "Photoinduced luminescence from the noble metals and its enhancement on roughened surfaces," Phys. Rev. B **33**, 7923–7936 (1986).
2. T. Haug, P. Klemm, S. Bange, *et al.*, "Hot-electron intraband luminescence from single hot spots in noble-metal nanoparticle films," Phys. Rev. Lett. **115**, 067403 (2015).
3. G. C. Li, Y. L. Zhang, J. Jiang, *et al.*, "Metal-substrate-mediated plasmon hybridization in a nanoparticle dimer for photoluminescence line-width shrinking and intensity enhancement," ACS Nano **11**, 3067–3080 (2017).
4. W. Rao, Q. Li, Y. Wang, *et al.*, "Comparison of photoluminescence quantum yield of single gold nanobipyramids and gold nanorods," ACS Nano **9**, 2783–2791 (2015).
5. S. Wang and T. Ding, "Photothermal-assisted optical stretching of gold nanoparticles," ACS Nano **13**, 32–37 (2019).
6. A. Babynina, M. Fedoruk, P. Kuhler, *et al.*, "Bending gold nanorods with light," Nano Lett. **16**, 6485–6490 (2016).
7. S. V. Makarov, A. S. Zalogina, M. Tajik, *et al.*, "Light-induced tuning and reconfiguration of nanophotonic structures," Laser Photon. Rev. **11**, 1700108 (2017).
8. A. Kuhlicke, S. Schietinger, C. Matyssek, *et al.*, "*In situ* observation of plasmon tuning in a single gold nanoparticle during controlled melting," Nano Lett. **13**, 2041–2046 (2013).
9. Q. Dai, M. Ouyang, W. Yuan, *et al.*, "Encoding random hot spots of a volume gold nanorod assembly for ultralow energy memory," Adv. Mater. **29**, 1701918 (2017).
10. S. Li, M. Panmai, S. Tie, *et al.*, "Regulating disordered plasmonic nanoparticles into polarization sensitive metasurfaces," Nanophotonics **10**, 1553–1563 (2021).
11. Y. H. Fu, A. I. Kuznetsov, A. E. Miroshnichenko, *et al.*, "Directional visible light scattering by silicon nanoparticles," Nat. Commun. **4**, 1527 (2013).
12. J. Xiang, J. Chen, Q. Dai, *et al.*, "Modifying Mie resonances and carrier dynamics of silicon nanoparticles by dense electron-hole plasmas," Phys. Rev. Appl. **13**, 014003 (2020).
13. H. Huang, F. Deng, J. Xiang, *et al.*, "Plasmon-exciton coupling in dielectric-metal hybrid nanocavities with an embedded two-dimensional material," Appl. Surf. Sci. **542**, 148660 (2021).
14. F. Deng, H. Huang, J. D. Chen, *et al.*, "Greatly enhanced plasmon-exciton coupling in Si/WS_2/Au nanocavities," Nano Lett. **22**, 220–228 (2022).
15. S. Liu, F. Deng, W. Zhuang, *et al.*, "Optical introduction and manipulation of plasmon-exciton-trion coupling in a Si/WS_2/Au nanocavity," ACS Nano **16**, 14390–14401 (2022).
16. C. Zhang, Y. Xu, J. Liu, *et al.*, "Lighting up silicon nanoparticles with Mie resonances," Nat. Commun. **9**, 2964 (2018).
17. J. Xiang, M. Panmai, S. Bai, *et al.*, "Crystalline silicon white light sources driven by optical resonances," Nano Lett. **21**, 2397–2405 (2021).
18. X. He, S. Liu, S. Li, *et al.*, "Si/Au hybrid nanoparticles with highly efficient nonlinear optical emission: implication for nanoscale white light sources," ACS Appl. Nano Mater. **5**, 10676–10685 (2022).
19. L. Zhou, M. Panmai, S. Li, *et al.*, "Lighting up Si nanoparticle arrays by exploiting the bound states in the continuum formed in a Si/Au hybrid nanostructure," ACS Photon. **9**, 2991–2999 (2022).
20. M. Panmai, J. Xiang, S. Li, *et al.*, "Highly efficient nonlinear optical emission from a subwavelength crystalline silicon cuboid mediated by supercavity mode," Nat. Commun. **13**, 2749 (2022).
21. J. Xiang, S. Jiang, J. Chen, *et al.*, "Hot-electron intraband luminescence from GaAs nanospheres mediated by magnetic dipole resonances," Nano Lett. **17**, 4853–4859 (2017).
22. C. H. Cho, C. O. Aspetti, J. Park, *et al.*, "Silicon coupled with plasmon nanocavity generates bright visible hot-luminescence," Nat. Photonics **7**, 285–289 (2013).
23. A. Ashkin, J. M. Dziedzic, J. E. Bjorkholm, *et al.*, "Observation of a single-beam gradient force optical trap for dielectric particles," Opt. Lett. **11**, 288–290 (1986).
24. A. Ashkin, "Optical trapping and manipulation of neutral particles using lasers," Proc. Natl. Acad. Sci. USA **94**, 4853–4860 (1997).
25. L. Gong, B. Gu, G. Rui, *et al.*, "Optical forces of focused femtosecond laser pulses on nonlinear optical Rayleigh particles," Photon. Res. **6**, 138–143 (2018).
26. K. Koshelev, S. Kruk, E. Melik-Gaykazyan, *et al.*, "Subwavelength dielectric resonators for nonlinear nanophotonics," Science **367**, 288–292 (2020).
27. L. Zhu, Y. Tai, H. Li, *et al.*, "Multidimensional optical tweezers synthetized by rigid-body emulated structured light," Photon. Res. **11**, 1524–1534 (2023).
28. E. M. Conwell, "Properties of silicon and germanium," Proc. IRE **40**, 1327–1337 (1952).
29. A. Rudenko, K. Ladutenko, S. Makarov, *et al.*, "Photogenerated free carrier-induced symmetry breaking in spherical silicon nanoparticle," Adv. Opt. Mater. **6**, 1701153 (2018).
30. I. Sinev, I. Iorsh, A. Bogdanov, *et al.*, "Polarization control over electric and magnetic dipole resonances of dielectric nanoparticles on metallic films," Laser Photon. Rev. **10**, 799–806 (2016).
31. E. Xifré-Pérez, L. Shi, U. Tuzer, *et al.*, "Mirror-image-induced magnetic modes," ACS Nano **7**, 664–668 (2013).
32. H. Li, Y. Xu, J. Xiang, *et al.*, "Exploiting the interaction between a semiconductor nanosphere and a thin metal film for nanoscale plasmonic devices," Nanoscale **8**, 18963–18971 (2016).
33. A. E. Miroshnichenko, A. B. Evlyukhin, Y. S. Kivshar, *et al.*, "Substrate-induced resonant magnetoelectric effects for dielectric nanoparticles," ACS Photon. **2**, 1423–1428 (2015).
34. G. P. Zograf, M. I. Petrov, S. V. Makarov, *et al.*, "All-dielectric thermonanophotonics," Adv. Opt. Photon. **13**, 643–702 (2021).
35. U. Zywietz, A. B. Evlyukhin, C. Reinhardt, *et al.*, "Laser printing of silicon nanoparticles with resonant optical electric and magnetic responses," Nat. Commun. **5**, 3402 (2014).
36. M. J. Crow, K. Seekell, and A. Wax, "Polarization mapping of nanoparticle plasmonic coupling," Opt. Lett. **36**, 757–759 (2011).
37. M. E. Kleemann, J. Mertens, X. Zheng, *et al.*, "Revealing nanostructures through plasmon polarimetry," ACS Nano **11**, 850–855 (2017).